PHYSICAL REVIEW A **83**, 012502 (2011)

High-precision frequency measurement of the 423-nm Ca I line

E. J. Salumbides,* V. Maslinskas, I. M. Dildar,† A. L. Wolf, E.-J. van Duijn, K. S. E. Eikema, and W. Ubachs‡
Institute for Lasers, Life and Biophotonics Amsterdam, VU University, De Boelelaan 1081, 1081 HV Amsterdam, The Netherlands
(Received 31 August 2010; published 7 January 2011)

We have performed an accurate frequency calibration of the $4s^2\,{}^1S_0 \rightarrow 4s4p\,{}^1P_1$ principal resonance line of the neutral calcium atom at 423 nm. Doppler-free cw excitation on a Ca atomic beam was performed by utilizing a Sagnac geometry in the alignment of the excitation beams. From frequency calibrations against a frequency comb, stabilized to a global positioning system (GPS) disciplined Rb standard, the transition frequency is determined at 709 078 373.01(35) MHz for the main ^{40}Ca isotope. Slightly lower accuracies are obtained for the transition frequencies of the less abundant isotopes. The achieved fractional uncertainty of 5×10^{-10} exceeds the requirements for including this transition in investigations that aim to probe a possible variation in the fine-structure constant α on cosmological time scales.

DOI: 10.1103/PhysRevA.83.012502 PACS number(s): 32.30.−r, 98.62.Ra, 42.62.Fi, 42.62.Eh

I. INTRODUCTION

The Ca I resonance line at 423 nm was already identified in the early days of spectroscopy as the Fraunhofer g line in the solar spectrum, and it still remains important for a number of applications in physics and astronomy. The recent searches for a possible variation of the fine-structure constant $\alpha = e^2/(4\pi\epsilon_0\hbar c)$ on a cosmological time scale are based on the many-multiplet (MM) method [1]. The MM method critically depends on a highly accurate determination of the transition frequencies of a number of principal resonance lines of metal elements in their neutral and ionized forms [2]. Inspired by the prospect of uncovering such a phenomenon, we have systematically measured accurate laboratory transition frequencies of metal lines that have been observed in quasar absorbers at high redshift. After the calibration of resonance lines in C [3], N [4], Mg [5,6], O [7], and Ca II [8], we now present the results of our measurements of the Ca I resonance line.

II. EXPERIMENT

A schematic representation of the experimental setup is shown in Fig. 1. An effusive beam of calcium atoms is produced from an oven that is heated by shining up to 20 W of 1064-nm laser radiation onto a metal receptacle containing calcium. The oven was operated at a sufficiently high temperature (∼900 K) to obtain spectroscopic signals from the less abundant Ca isotopes. Two skimmers (with 1-mm radius and 90-cm separation) downstream serve to produce a collimated atomic beam with a divergence of ∼1 mrad.

The excitation laser beam is produced by frequency doubling the output of a cw Ti:sapphire laser with the fundamental wavelength $\lambda_{\rm fund} \sim 846$ nm. A LiB_3O_5 (LBO) crystal ($\phi = 25^\circ$) was used as the nonlinear medium inside an enhancement cavity generating ∼40 mW of 423-nm light. A collimated excitation beam with a diameter of ∼2.5 mm is used in the spectroscopic investigations. Neutral density filters were used to attenuate the excitation intensity so that most of the measurements could be performed at low intensities, except when investigating systematic effects. As the atoms decay back to the ground state from the $^1P_1$ state (lifetime ∼4.6 ns) after the laser excitation, the fluorescence is collected onto a photomultiplier tube and recorded as the spectroscopic signal.

To compensate for first-order Doppler shifts, the excitation beam was split into two paths and made to overlap in counter-propagating directions. The counter-propagating laser beams cross the Ca atomic beam at a (near) perpendicular orientation, where the effect of (residual) Doppler broadening is least. To ensure the best alignment of the counter-propagating laser beams, a Sagnac interferometric technique is used [9].

For calibration purposes, a fraction of the output of the cw Ti:sapphire laser is mixed with the output of a frequency-comb laser that is locked to a global positioning system (GPS) disciplined Rb clock standard. We have used both a Ti:sapphire-based frequency-comb laser and an Er-doped fiber frequency-comb laser, operated at different repetition frequencies ($f_{\rm rep}$) in the frequency calibration (see later discussion on the mode-number determination).

III. RESULTS AND DISCUSSION

We have performed frequency calibrations of the $4s^2\,{}^1S_0 \rightarrow 4s4p\,{}^1P_1$ transition for all naturally occurring Ca isotopes ^{40}Ca, ^{42}Ca, ^{43}Ca, ^{44}Ca, and ^{48}Ca, except for ^{46}Ca, which is the least abundant. The natural abundances of the ^{40}Ca, ^{42}Ca, ^{43}Ca, ^{44}Ca, ^{46}Ca, and ^{48}Ca isotopes are 96.94(16)%, 0.65(2)%, 0.14(1)%, 2.09(11)%, 0.004(3)%, and 0.19(2)%, respectively [10]. Several absolute- and relative-frequency calibrations were carried out, resulting in the determination of the respective isotope shifts. We have performed absolute-frequency calibrations on the main ^{40}Ca isotope to assess systematic ac Stark and Zeeman shifts. These possible sources of systematic shifts are discussed in the following.

A. Doppler shift

For each frequency determination, recordings of the spectrum are performed using each of the counter-propagating

*e.j.salumbides@vu.nl; also at the Department of Physics, University of San Carlos, Cebu 6000, Philippines.
†Present address: Kamerlingh Onnes Laboratory, Leiden Institute of Physics, P.O. Box 9504, NL-2300 RA Leiden, The Netherlands.
‡w.m.g.ubachs@vu.nl

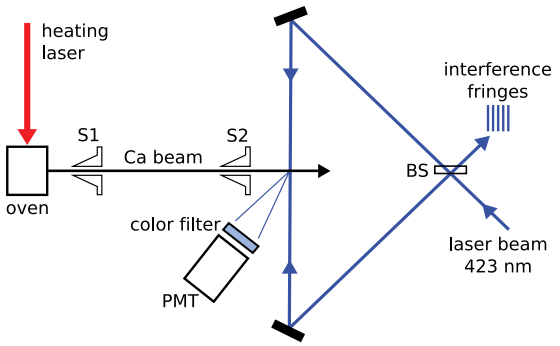

FIG. 1. (Color online) Experimental setup. Skimmed Ca atomic beams are crossed with counter-propagating laser beams in Sagnac geometry. (S1 and S2 are skimmers and BS is the beamsplitter.) The laser-induced fluorescence is collected onto a photomultiplier tube (PMT).

laser beams separately. When using the Sagnac geometry, the Doppler shift of the transition frequency obtained for each beam will have the same magnitude but opposite signs, so the average of the transition-center frequency results in a cancellation of the first-order Doppler shifts [9]. Figure 2 shows separate recordings of the counter-propagating laser beams, illustrating the oppositely directed shifts of the peak positions for ^{40}Ca. A misalignment in the counter-propagating excitation beams will result in a difference in magnitude of the Doppler shifts for the respective beams. From the Sagnac interferometric alignment technique, we give a conservative misalignment estimate of 0.1 mrad. This causes a residual Doppler shift as a result of a possible imperfect cancellation of about 170 kHz.

Also shown in Fig. 2 is the fitted Lorentzian function, where the peak-frequency position can be determined to be better than 0.1% of the linewidth. The weighted average of the results from Refs. [11–13] for the lifetime of the excited $^1P_1$ state is $\tau = 4.60(14)$ ns. This lifetime translates to a natural linewidth

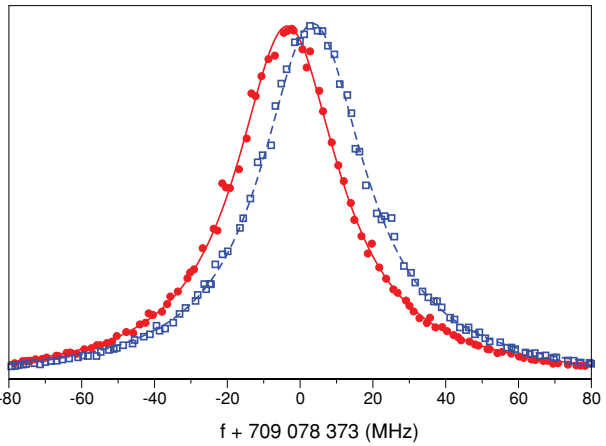

FIG. 2. (Color online) Spectra obtained for the counter-propagating laser beams. The laser beams were purposely misaligned slightly from being perpendicular with respect to the atomic beam to demonstrate the Doppler shifts of opposite signs for the exactly aligned counter-propagating beams.

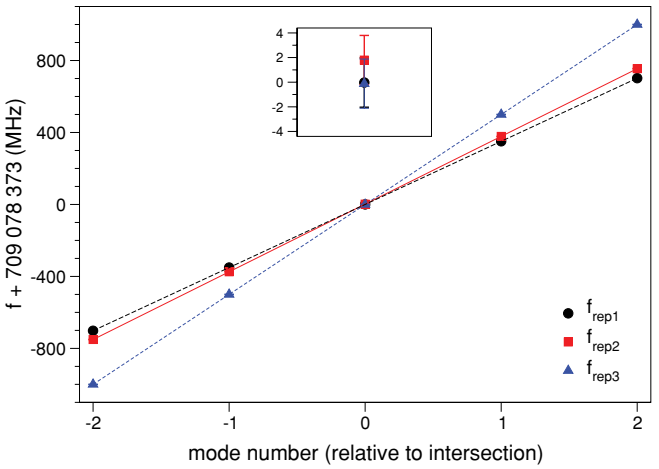

FIG. 3. (Color online) The determination of the correct mode number (shifted to $n = 0$) is achieved by performing measurements on the ^{40}Ca transition frequency using three different $f_{\rm rep}$ values: $f_{\rm rep1} \sim 175$ MHz, $f_{\rm rep2} \sim 188$ MHz, and $f_{\rm rep3} \sim 250$ MHz. Lines are drawn through the different $f_{\rm rep}$ sets to guide the eye. (Inset) The coincidence of the transition frequency, obtained using the different $f_{\rm rep}$ values, at the correct mode number.

of 34.6(1.1) MHz, which is in good agreement with that obtained from this investigation.

B. Frequency-comb calibration

In the absolute-frequency calibration, the fundamental frequency $f_{\rm cw}$ from a cw Ti:sapphire ring laser is mixed with the frequency-comb radiation, and the beat frequency $f_{\rm beat}$ is counted. The fundamental frequency $f_{\rm cw}$ is then obtained by the simple relation $f_{\rm cw} = nf_{\rm rep} + f_0 + f_{\rm beat}$, where $f_{\rm rep}$ and f_0 are the repetition and offset frequencies of the frequency comb, respectively (in practice, the signs of f_0 and $f_{\rm beat}$ may be negative and need to be determined). Note that the second harmonic of $f_{\rm cw}$ is used in the spectroscopic investigations; therefore, $f_{\rm cw}$ has to be multiplied by a factor of 2 to obtain the transition frequencies. The integer mode number n must be determined from independent means, usually from a previous measurement if the accuracy is better than half of $f_{\rm rep}$. However, the accuracy obtained from the classical spectroscopy of Risberg [14] ($\Delta f_{\rm cw} = 300/2$ MHz; see Table III) is not adequate for an unambiguous determination of the mode-number. The method we used to resolve the mode-number determination is similar to that used in Refs. [8,15,16], that is, by performing calibrations of the ^{40}Ca transition frequencies using sufficiently different values of $f_{\rm rep}$. In Fig. 3, we plot the resulting $f_{\rm cw}$ as a function of n for measurements obtained from using different values for the frequency-comb $f_{\rm rep}$. We have used a Ti:sapphire frequency comb with $f_{\rm rep1} \sim 175$ MHz and $f_{\rm rep2} \sim 188$ MHz for the first two sets, while another fiber frequency comb with $f_{\rm rep3} \sim 250$ MHz was used for the last set of measurements. The correct n is inferred to be that value where the measurements from the three sets of $f_{\rm rep}$ values coincide (the mode-number axis is shifted so that $n = 0$ is the coincidence point). The inset zooms in on the intersection region, which demonstrates how well the transition-frequency values coincide, most notably

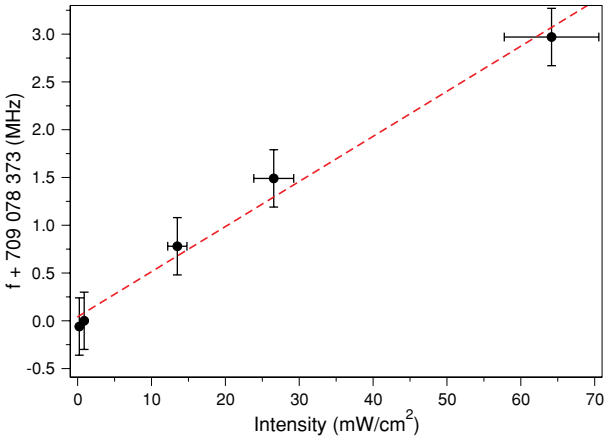

FIG. 4. (Color online) The ac Stark shift is determined by measuring the transition frequency at different intensities.

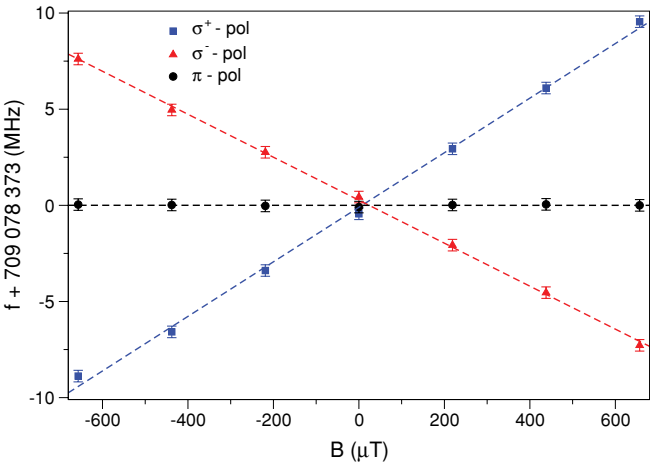

FIG. 5. (Color online) Possible Zeeman shifts were assessed by performing spectroscopy with circular (σ^+ and σ^-) and linear (π) polarizations of the excitation laser in the presence of an applied magnetic field B.

for the f_{rep1} and f_{rep3} datasets. The value obtained when using f_{rep2} is off with respect to the other two sets because the Stark shift was not taken into account since the purpose of this set of measurements is only to determine the correct mode-number. We note that the next coincidence-frequency values are several gigahertz away on either side, so that these coincidence values can be ruled out on the basis of the Risberg measurement [14] with a 300-MHz accuracy.

C. ac Stark and Zeeman shifts

Figure 4 displays a plot of the ^{40}Ca resonance frequency as a function of the excitation laser intensity. The ac Stark coefficient obtained is 47(3) kHz/(mW/cm^2) and the extrapolated intercept is 709 078 373.04 MHz, with a 100-kHz uncertainty from the fit. The widths of the transitions also broaden with increasing intensity (not shown in the plot), and we are able to extrapolate the natural linewidth (from the width at zero light intensity) to be 34.5(4) MHz. We note that, for the purpose of frequency calibration, it is sufficient to extrapolate the ac Stark shift from relative intensity measurements. Nevertheless, we have estimated the intensity from the measured power and the beam cross section, where we have neglected inhomogeneous effects in order to extract values for the ac Stark shift coefficient, as well as the saturation intensity, for comparison. We obtain a saturation intensity (at resonance) I_s of 54(5) mW/cm^2 from the linewidth-intensity relation, which is in agreement with the calculated value [$I_s = \pi hc/(3\lambda^3\tau)$] for this transition of 60(2) mW/cm^2. The frequency calibrations of the main ^{40}Ca isotope have been performed multiple times at low intensities, which are typically $\sim(1/400)I_s$, resulting in negligible ac Stark shifts.

To investigate possible Zeeman shifts, we performed the measurements of the ^{40}Ca resonance frequency in the presence of applied magnetic fields. In the first set of measurements, we used circularly polarized light (σ^+ and σ^-), with the direction of the applied magnetic field in the same axis as the excitation-beam propagation. In the second set of measurements, we used linearly polarized light (π), where the electric field vector is parallel to the applied magnetic-field direction. For the measurements with circularly polarized excitation beams, a $\lambda/4$ waveplate was placed before the beamsplitter that was used for the Sagnac alignment. The beam transmitted through the polarizer represents the σ^+ component, while the reflected beam is the σ^- component. The magnetic field is generated from a pair of coils, and the field magnitude in the interaction region was varied up to 660 μT. Figure 5 shows the frequency shifts against the applied magnetic field for the respective polarizations.

In the presence of a magnetic field, the energies of the m sublevels of the Ca $^1P_1$ state split apart, while the $^1S_0$ state remains unchanged. Transitions to the $m = 1$ and $m = -1$ sublevels are accessed by using light with σ^+ and σ^- polarizations, respectively, while the transition to the $m = 0$ sublevel is accessed with π polarization. In the low-magnetic-field regime, the Zeeman shift of the $m = 1$ energy level is calculated to be $\sim$14 kHz/μT (~ -14 kHz/μT for the $m = -1$ energy level), while the $m = 0$ energy level does not shift. We have fitted a line through the measured data points and obtained the slope of $-14.2(5)$ kHz/μT for the σ^+ dataset and a slope of $-11.2(5)$ kHz/μT for the σ^- dataset. This indicates that the σ^- polarization is not pure and has about 20% residual σ^+ polarization component. (Note that the σ^- polarization beam is the reflection off a beamsplitter that is not optimized to preserve the polarization components.) This is also supported by the observation that the linewidth is broader for the σ^- dataset at the highest applied magnetic-field strengths, while no broadening is observed for the σ^+ dataset. As expected, the π polarization dataset does not exhibit any Zeeman shift. The value of the applied B field, where the σ^+ and σ^- datasets cross, is 14(3) μT. This residual field is close to the Earth's magnetic-field horizontal component of $\sim$19 μT. The orientation of the experimental setup is such that the influence of the north-south and east-west components is negligible.

The absolute calibrations of the transition frequency were performed using linearly polarized excitation beams at zero applied magnetic field; therefore, no correction for the Zeeman shift is necessary. We can estimate an upper limit to a possible Zeeman shift in the case of imperfect linear polarization, where the fraction of σ^+ and σ^- components is not equal. In the conservative case of a 10% imbalance between the

TABLE I. Corrections and uncertainties for the ^{40}Ca transition frequency.

Source	Correction (kHz)	Uncertainty (kHz)
Residual Doppler	0	170
Second-order Doppler	−1	1
Recoil shift	−28	0
ac Stark shift	0	100
Zeeman shift	0	20
Line fitting	0	200
Statistical	0	200
Total	−29	350

σ components, we expect a residual Zeeman shift of ∼20 kHz at the residual field of 14(3) μT.

D. Uncertainty assessment

Based on the preceding discussions, we list the corrections to the transition frequency of the main ^{40}Ca isotope, as well as the corresponding uncertainty estimates, in Table I. The Doppler, recoil, ac Stark, and Zeeman shift entries represent systematic effects. The line-fitting uncertainty includes the following contributions: (1) the uncertainty in the peak-frequency determination that is proportional to the linewidth; (2) peak-frequency shifts induced by the background contribution from the other resonances that are not accurately taken into account; and (3) a contribution due to the signal-to-noise ratio (SNR) of the recording. The *statistical* uncertainty contribution represents the standard deviation of a set of transition-frequency values obtained from several measurements taken at identical conditions.

There are additional *systematic* uncertainty contributions for the transitions of the less abundant isotopes, mainly due to line fitting. Since we recorded a limited frequency interval in a single measurement, we opted to perform the line-fitting routines on separate lines representing the isotope transition. The strong background signal from the wing of the ^{40}Ca transition (see Fig. 6) was approximated as a linearly sloping background. This simple background fitting is then expected to lead to slight shifts in the line-center positions for the less abundant isotopes. This effect is even more severe in the case of the ^{43}Ca isotope when compared to the even isotopes, owing to the hyperfine splitting in ^{43}Ca, its low abundance, and its proximity to the ^{44}Ca line (second most abundant isotope). In general, the ^{40}Ca transition has the least line-fitting uncertainty contribution among the isotopes, since the ^{40}Ca line is the most intense, it has the best SNR, and the contribution of the wings of the less abundant isotopes is minimal. The ^{40}Ca table of uncertainties therefore indicates a lower limit in the accuracy of the absolute transition frequencies for the other less abundant Ca isotopes.

In Table I, the main uncertainty contribution of 200 kHz is from the line fitting, which is mostly due to the broad natural linewidth and small contributions from the fitting model (simplistic background fitting) and the measurement procedure used (limited frequency range for each measurement scan). The second largest contribution is from the residual Doppler shift, where we give a conservative estimate of 170 kHz. This can be improved with some effort, such as an implementation of an automated Sagnac-alignment adjustment to counteract drifts. However, this adjustment compensation is not crucial for this particular experiment, and it would be more relevant in cases where the natural linewidth of the transition is narrower. The error contribution from the ac Stark shift is obtained from the extrapolation of the transition frequency to zero excitation intensities. The Zeeman shift is a conservative estimate based on a possible imperfect linear polarization in the presence of the Earth's magnetic field. The recoil shift correction of −29 kHz was also applied to the value of the transition frequency, despite it being an order of magnitude smaller than the total uncertainty. By taking the corrections and uncertainties into account, we have determined the $4s^2\,{}^1S_0 \rightarrow 4s4p\,{}^1P_1$ transition frequency of ^{40}Ca to be 709 078 373.01(35) MHz.

TABLE II. Isotope shifts obtained from the experiment. Values are in megahertz.

Isotope	This work	Ref. [17][a]	Ref. [18]
^{42}Ca	393.1(4)	393.50(10)	391.1(8)
^{43}Ca (cg)[b]	610.7(6)	611.80(15)	611.0(10)
^{44}Ca	773.8(2)	773.80(15)	770.8(8)
^{48}Ca	1513.1(4)	1513.00(20)	1510.7(8)

[a]Uncertainty values listed here are half of the 2σ uncertainties quoted in Ref. [17].
[b]Center of gravity.

E. Isotope shifts

An overview scan showing the isotope shift of the Ca $4s^2\,{}^1S_0 \rightarrow 4s4p\,{}^1P_1$ transition is shown in Fig. 6. Except for the least abundant ^{46}Ca isotope, all naturally occurring Ca isotopes were detected. We have performed absolute- and relative-frequency calibrations of the transitions of these isotopes. The resulting line positions relative to the ^{40}Ca isotope are listed in Table II, where they are compared to the previous results of Nörtershäuser *et al.* [17] and Andl *et al.* [18]. The nuclear spin of the ^{43}Ca isotope is 7/2, causing

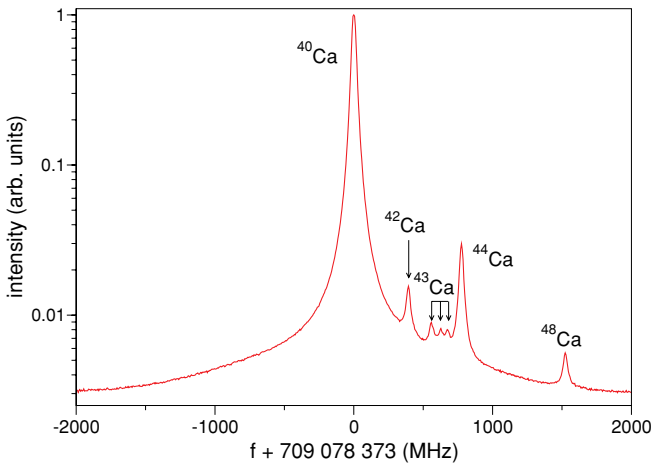

FIG. 6. (Color online) Overview spectrum showing the isotope shifts of the Ca $4s^2\,{}^1S_0 \rightarrow 4s4p\,{}^1P_1$ transition. All naturally occurring isotopes are detected except for the least abundant ^{46}Ca.

TABLE III. Transition energy of the main isotope ^{40}Ca and the center of gravity (cg) of the transition accounting for contributions from the other isotopes. The cg value can be compared to that obtained in the classical spectroscopy of Risberg [14], where the isotope shifts were not resolved.

Source	ν (cm^{-1})
This work: ^{40}Ca	23 652.308 592 (12)
This work: cg	23 652.309 337 (12)
Risberg: cg	23 652.304 (10)

the $4s^2\,{}^1S_0 \rightarrow 4s4p\,{}^1P_1$ transition to split into three hyperfine components ($m_F = 9/2,\ 7/2,\ 5/2$, in order of increasing transition frequencies). The isotopes with *even* atomic mass number, i.e., ^{40}Ca, ^{42}Ca, ^{44}Ca, and ^{48}Ca, have zero nuclear spins and consequently no hyperfine structure. The isotope shifts that we obtain are in good agreement with the previous results, except for the ^{43}Ca transition center of gravity (cg), which is slightly off from the results of Ref. [17].

F. Transition center of gravity

The transition wavelengths of Ca were determined by Risberg [14] using classical spectroscopy. To our knowledge, there has been no subsequent absolute-frequency calibration of this transition; in fact, the recent atomic data compilation by Sansonetti and Martin [19] still lists the Risberg value [14]. This is despite the prevalent use of the $4s^2\,{}^1S_0 \rightarrow 4s4p\,{}^1P_1$ as the cooling transition, e.g., in Ca atomic clocks [20] and in the trapping of the extremely rare ^{41}Ca isotope in a magneto-optical trap [21].

The transition energy of the $4s^2\,{}^1S_0 \rightarrow 4s4p\,{}^1P_1$ transition of the main ^{40}Ca isotope is listed in Table III. We also list the center-of-gravity value calculated from the isotope shifts weighted by the respective isotope abundances. This cg transition value can be compared to the previous determination of Risberg [14], where the accuracy of the present value represents more than an 800-fold improvement.

G. Sensitivity coefficient for α-variation

The sensitivity coefficient q for α-variation of the Ca $4s^2\,{}^1S_0 \rightarrow 4s4p\,{}^1P_1$ transition was calculated by Flambaum and Dzuba [22] to be $q = 250$. Taking the value for the α-variation as $\delta\alpha/\alpha = (-0.543 \pm 0.116) \times 10^{-5}$ [1], we calculate a blueshift in this resonance line of 81(17) MHz when compared to the transition frequency of $\sim$10 billion years ago. Isotope abundances in some stars seem to be stratified, so that the lighter isotopes tend to be closer to the core in these systems [23]; therefore, it is not unlikely that the Ca abundance ratios in space are different from those on Earth. If the heavier isotopes ^{46}Ca and ^{48}Ca have 20 times the terrestrial abundance (and lesser ^{40}Ca abundance), the center of gravity for these transitions would shift by $\sim$80 MHz, an effect that is of the same order of magnitude and sign as that caused by the α-variation claimed in Ref. [1]. Isotopic shifts from different Ca I (and Ca II) transitions with different q-values might be used in future studies to distinguish a shift caused by different isotopic abundances and a shift caused by α-variation.

IV. CONCLUSIONS

We have determined the transition frequency of the main resonance in ^{40}Ca and its isotopes ^{42}Ca, ^{43}Ca,^{44}Ca, and ^{48}Ca. The achieved accuracy of the derived transition energy center of gravity represents an almost three-orders-of-magnitude improvement over previous results from classical spectroscopy [14]. If the isotopic abundances can be established to be identical to the terrestrial abundance values, we recommend the use of the transition-energy cg of 23 652.309 337 (12) cm^{-1}. The isotopic shifts measured in this study are in agreement with previous high-resolution studies [17]. With a fractional uncertainty of $\sim 5 \times 10^{-10}$ in the present determination, this transition Ca I frequency may be included in the MM method to search for a possible variation in the fine-structure constant α.

ACKNOWLEDGMENTS

This work was financially supported by the Netherlands Foundation for Fundamental Research (FOM) and by the Smart Mix Program MEMPHIS of the Netherlands Ministry of Economic Affairs and the Netherlands Ministry of Education, Culture and Science. V.M. acknowledges support from the EU Erasmus program and I.M.D. acknowledges support from the Pakistan Higher Education Commission (HEC).

[1] M. T. Murphy, J. K. Webb, and V. V. Flambaum, Mon. Not. R. Astron. Soc. **345**, 609 (2003).
[2] J. C. Berengut and V. V. Flambaum, Hyperfine Interact. **196**, 269 (2010).
[3] I. Labazan, E. Reinhold, W. Ubachs, and V. V. Flambaum, Phys. Rev. A **71**, 040501 (2005).
[4] E. J. Salumbides, J. P. Sprengers, E. Reinhold, and W. Ubachs, J. Phys. B **38**, L383 (2005).
[5] S. Hannemann, E. J. Salumbides, S. Witte, R. T. Zinkstok, E.-J. van Duijn, K. S. E. Eikema, and W. Ubachs, Phys. Rev. A **74**, 012505 (2006).
[6] E. J. Salumbides, S. Hannemann, K. S. E. Eikema, and W. Ubachs, Mon. Not. R. Astron. Soc. **373**, L41 (2006).
[7] T. I. Ivanov, E. J. Salumbides, M. O. Vieitez, P. C. Cacciani, C. A. de Lange, and W. Ubachs, Mon. Not. R. Astron. Soc. **389**, L4 (2008).
[8] A. L. Wolf, S. A. van den Berg, C. Gohle, E. J. Salumbides, W. Ubachs, and K. S. E. Eikema, Phys. Rev. A **78**, 032511 (2008).
[9] S. Hannemann, E. J. Salumbides, and W. Ubachs, Opt. Lett. **32**, 1381 (2007).
[10] J. R. de Laeter, J. K. Böhlke, P. de Bièvre, H. Hidaka, H. S. Peiser, K. J. R. Rosman, and P. D. P. Taylor, Pure Appl. Chem. **75**, 683 (2003).
[11] A. Lurio, R. L. deZafra, and R. J. Goshen, Phys. Rev. **134**, A1198 (1964).

[12] W. W. Smith and A. Gallagher, Phys. Rev. **145**, 26 (1966).
[13] E. Hulpke, W. Paul, and E. Paul, Z. Phys. **177**, 257 (1964).
[14] G. Risberg, Ark. Fys. **37**, 231 (1968).
[15] L.-S. Ma, M. Zucco, S. Picard, L. Robertsson, and R. Windeler, IEEE J. Sel. Top. Quantum Electron. **9**, 1066 (2003).
[16] S. Witte, R. T. Zinkstok, W. Ubachs, W. Hogervorst, and K. S. E. Eikema, Science **307**, 400 (2005).
[17] W. Nörtershäuser, N. Trautmann, K. Wendt, and B. A. Bushaw, Spectrochim. Acta B **53**, 709 (1998).
[18] A. Andl, K. Bekk, S. Göring, A. Hanser, G. Nowicki, H. Rebel, G. Schatz, and R. C. Thompson, Phys. Rev. C **26**, 2194 (1982).
[19] J. Sansonetti and W. Martin, J. Phys. Chem. Ref. Data **34**, 1559 (2005).
[20] G. Wilpers *et al.*, Metrologia **44**, 146 (2007).
[21] S. Hoekstra, A. Mollema, R. Morgenstern, L. Willmann, H. Wilschut, and R. Hoekstra, Hyperfine Interact. **162**, 167 (2005).
[22] V. V. Flambaum and V. A. Dzuba, Can. J. Phys. **87**, 25 (2009).
[23] T. Ryabchikova, O. Kochukhov, and S. Bagnulo, Astron. Astrophys. **480**, 811 (2008).